

The elliptical model of two-dimensional vortex dynamics. I: The basic state

Bernard Legras

Laboratoire de Météorologie Dynamique du CNRS, École Normale Supérieure, 24 rue Lhomond, 75231 Paris Cedex 05, France

David G. Dritschel

Department of Applied Mathematics and Theoretical Physics, University of Cambridge, Silver Street, Cambridge CB3 9EW, England

(Received 6 February 1990; accepted 6 December 1990)

An approximate model of nonaxisymmetric vortices in a two-dimensional fluid is developed in which each vortex is assumed to consist of a nested stack of elliptical regions of uniform vorticity. The model is governed by a set of coupled nonlinear ordinary differential equations for the aspect ratio, orientation, and centroid of the bounding contour of each region. It also admits a Hamiltonian formulation and possesses all the invariants of the original system. In Part II [Phys. Fluids A 3, 855 (1991)], the model is extended to include disturbances to the elliptical shape of each contour.

I. INTRODUCTION

It is now widely recognized that coherent vortices are the dominant feature of a very broad class of incompressible two-dimensional inertial flows with high Reynolds number. These structures are spontaneously generated in decaying turbulence with arbitrary initial conditions^{1,2} or in forced turbulence with either deterministic or random forcing.³ Their leading role was initially discovered within numerical simulations⁴⁻⁶ and confirmed more recently within numerous experiments in real fluids (e.g., Refs. 7-11).

A significant amount of work has been devoted to the study of the stability of coherent vortices. It is, however, generally assumed that the basic vorticity profile is axisymmetric, a case for which the Euler equations are trivially satisfied. Many fewer results are available that deal with nonaxisymmetric structures, and most of these latter have been obtained only for patches of finite area over which the vorticity is uniform. For vortex patches, the Lagrangian formalism of contour dynamics^{12,13} is a well-adapted tool to describe the evolution of the patches and to obtain exact nonaxisymmetric equilibrium figures with one or several patches.¹³⁻¹⁶ The simple figure of a single elliptical vortex, due to Kirchhoff, is an exact analytical solution of the Euler equations (Ref. 17, Art. 159), and one for which the effect of external shear or strain can be easily taken into account.^{18,19} In the absence of shear or strain, the ellipse rotates with a constant angular velocity while maintaining a fixed aspect ratio. In the presence of shear or strain, the ellipse may oscillate while changing its aspect ratio.

A particularly important extension to the solution for a single ellipse is the second-order moment model of Melander *et al.*²⁰ (hereafter denoted as MZS). These authors consider the interaction between several Kirchhoff ellipses and obtain a self-consistent model in which the aspect ratio and the orientation of each elementary elliptical vortex vary in response to the self-induced velocity field and that of other vortices. In reality, the elliptical shape of each vortex is not strictly preserved under the temporal evolution. Indeed the model is based on a second-order truncation of an expansion

that describes each patch by its vorticity, the position of its centroid, and a series of moments with respect to its centroid. This truncation gives good results as long as the vortices remain far apart. The model has been used to determine multipolar solutions and also has provided a simple criterion for symmetric vortex merging that falls within 10% of direct measurements.

While sharp external boundaries (such as that characteristic of an elliptical patch) are really observed as a result of the stripping of low-lying vorticity from vortex edges by an external straining flow,^{21,22} the restriction to vortices with entirely uniform vorticity is a serious limitation to our understanding of two-dimensional flows. However, apart from a few exceptions, such as the Lamb dipole,²³ nonaxisymmetric, distributed solutions of the Euler equations have eluded straightforward analysis.

Only recently, contour dynamics has been applied to distributed vortices, uncovering a variety of stationary, translating, and rotating solutions with up to several tens of layers.¹³ The monopolar, single vortex solutions obtained in this way exhibit vorticity contours that are very close to ellipses even when the aspect ratio is small; a similar observation had already been made previously in axisymmetrization experiments using a continuous distribution of vorticity.²⁴ It is thus natural to attempt to extend the approach followed by MZS to the dynamics of a distributed region of vorticity with elliptical contours. This, however, requires a radical rethinking of the problem because the method used by MZS is basically designed for distant vortices and cannot be used here to make the required analytical calculations. The purpose of this paper is to present a new approach based on conformal transforms and complex integration that exactly extracts the part of the motion preserving each contour's elliptical shape. This method is able to handle both cases of embedded and separated contours. In the following paper,²⁵ we allow for small departures from the elliptical contour shape and we apply the extended model to the stability of nonaxisymmetric solutions and to the merging of vortices, with surprising success.

Section II presents the basic assumptions of the model and discusses the kinematics of evolving ellipses. We obtain an equation relating the evolution of the parameters of each vorticity contour to the leading coefficients of a trigonometric expansion of the normal velocity along this contour. The following four sections, Secs. III–VI, show how these coefficients can be calculated exactly, without any further assumption, for the four types of velocity fields acting, in our model, on an elementary elliptical vortex with uniform vorticity. The ordering of these sections follows the increasing complexity of the calculation, beginning with the effect of an external straining flow in Sec. III, proceeding to the action of an external embedding elliptical vortex in Sec. IV, then to the action of an internal embedded elliptical vortex in Sec. V, and finishing with the effect of a separated elliptical vortex in Sec. VI. Section VII summarizes the results by giving the elementary Hamiltonian for each interaction involved in the model and establishes that the model possesses all the invariants of the original equations. Some concluding remarks are offered in Sec. VIII.

II. THE ELLIPTICAL ASSUMPTION

We consider any vortex or distribution of vortices that can be built up from a superposition of vorticity disks (Fig. 1). Each disk, labeled with j , has area A_j and vorticity ω_j , both of which are conserved through the temporal evolution. The initial shape of each disk is elliptical with semimajor and semiminor axis lengths a_j and b_j , respectively. The aspect ratio is $\lambda_j \equiv b_j/a_j$ and the orientation ϕ_j of the ellipse is the angle between the principal axis and an arbitrary reference axis. The center of the disk (X_j, Y_j) is denoted by the complex variable $Z_j = X_j + iY_j$. Figure 1 shows the case of a single vortex with a monotonic profile of vorticity, but it is clear that several separated vortices can be described the same way and that nonmonotonic profiles can be obtained using a distribution of positive and negative values for ω_j . Owing to incompressibility and conservation of vorticity, the evolution of each disk is entirely described by the deformation of its boundary under its own action and the action of other disks. In addition we allow the vortex to be immersed

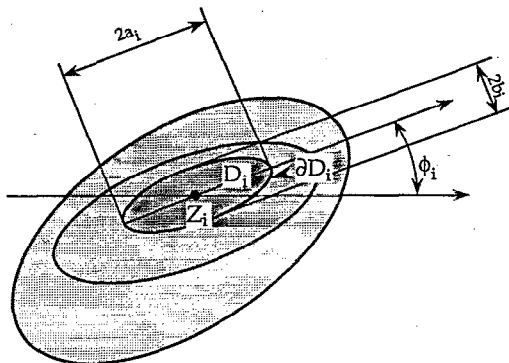


FIG. 1. Structure of an elliptical vortex. The vortex is built as a superposition of vorticity disks. Each disk D_i of boundary ∂D_i is described by its vorticity ω_i , its centroid Z_i , its orientation ϕ_i , and its semimajor and semiminor axes a_i and b_i .

in a uniform external straining flow having arbitrary strain and background rotation rates.

The basic assumption of the model is that disks stay elliptical during the temporal evolution, that is, the evolution is fully described by the variations of $Z_j(t)$, $\lambda_j(t)$, and $\phi_j(t)$. We also assume that the boundaries of the disks do not cross. Unlike MZS, our model is not based directly on a moment expansion of the vorticity distribution. This formulation leads MZS to use a Taylor expansion of the velocity field around the center of each disk, resulting in estimates for the second (elliptical) moments which deviate more and more from their true values as the aspect ratio decreases. (This discrepancy is very sensible for the case of self-advection and the interaction of superimposed disks. It is much less important in the case of distant patches of vorticity studied by MZS. Furthermore, MZS avoids the problem of self-advection by using the exact solution that is known for an isolated elliptical patch of uniform vorticity.) We compute, instead, the exact contribution to the deformation of each disk boundary that preserves the elliptical shape (but shifts the center, rotates the disk, and changes the aspect ratio). The neglected terms lead to higher-order nonelliptical deformations; they give no contribution to the second-order moments. We shall show that this approximation corresponds, indeed, to a truncation of the normal velocity field on each contour to the first two terms of an expansion in the elliptical azimuthal coordinate.

The evolution of each disk boundary arises from five contributions: the first is due to the external straining flow, the second is due to the external disks belonging to the same vortex, the third is self-advection, the fourth is due to the interior disks, and the fifth is due to other vortices. As we shall see shortly, the first three contributions exactly preserve the disk's elliptical shape while the fourth and the fifth give rise to higher-order deformations. The fourth and the fifth are also the most difficult to compute.

For a given elliptical disk of vorticity, centered at the location Z , it is convenient to define the associated system of elliptical coordinates $w = \xi + i\eta$ as

$$z = Z + e^{i\phi} c \cosh w, \quad (1)$$

where $z = x + iy$ is the complex Cartesian coordinate, ϕ is the orientation of the disk with respect to the x axis, and

$$c = \sqrt{a^2 - b^2} = \sqrt{(1/\lambda - \lambda)A/\pi}$$

is the distance of each focus from the origin. In this system, the coordinate lines are a family of orthogonal confocal ellipses and hyperbolas, where the radial coordinate ξ parametrizes the ellipses and the azimuthal coordinate η parametrizes the hyperbolas (see Ref. 17, Art. 66 or Ref. 26, p. 502).

We also use the complex Cartesian coordinate \bar{z} linked to the principal axis of the ellipse:

$$\bar{z} = c \cosh w. \quad (2)$$

Note that z is a coordinate in the fixed reference frame while \bar{z} and w are attached to a moving and deforming disk of vorticity.

The velocity of a given material point with coordinate z is given by

$$\dot{z} = i \left(\frac{\partial \psi}{\partial z} \right)^*, \quad (3)$$

where ψ is the streamfunction (here defined as a real function in the complex plane) and * denotes conjugation. In the time-evolving elliptical coordinates of a given disk, Eqs. (1) and (3) give

$$\dot{Z}e^{-i\phi} + \dot{c} \cosh w + c\dot{w} \sinh w = \frac{i}{c \sinh w^*} \left(\frac{\partial \psi}{\partial w} \right)^* - i\dot{\phi}c \cosh w. \quad (4)$$

Upon multiplying by $c \sinh w^*$ and taking the real \Re and imaginary \Im parts, we obtain

$$c \Re [\dot{Z}e^{-i\phi}] \sinh \xi \cos \eta + c \Im [\dot{Z}e^{-i\phi}] \cosh \xi \sin \eta + \frac{1}{2} c \dot{c} \sinh 2\xi + h^2 \dot{\xi} = - \frac{\partial \psi}{\partial \eta} - \frac{1}{2} \dot{\phi} c^2 \sin 2\eta, \quad (5)$$

$$c \Im [\dot{Z}e^{-i\phi}] \sinh \xi \cos \eta - c \Re [\dot{Z}e^{-i\phi}] \cosh \xi \sin \eta + \frac{1}{2} c \dot{c} \sin 2\eta + h^2 \dot{\eta} = + \frac{\partial \psi}{\partial \xi} + \frac{1}{2} \dot{\phi} c^2 \sinh 2\xi, \quad (6)$$

where the scale factor h^2 is given by

$$h^2 = c^2 |\sinh w|^2 = \frac{1}{2} c^2 (\cosh 2\xi - \cos 2\eta).$$

In Eqs. (5) and (6), we have assumed that the system of elliptical coordinates is changing with time under the evolution of the vorticity disk with which it is linked. The evolution of the elliptical coordinate system itself can be obtained from Eq. (5) by specializing it to the material points on the disk boundary and by applying the fundamental assumption of permanent elliptical shape. Denoting $\xi = \Gamma$ as the radial elliptical coordinate of the disk boundary, the first step of the approximation is to use conservation of disk area, $A \equiv \frac{1}{2} \pi c^2 \sinh 2\Gamma$, to obtain

$$\dot{\Gamma} = -(\dot{c}/c) \tanh 2\Gamma. \quad (7)$$

Replacing $\dot{\xi}$ by $\dot{\Gamma}$ in Eq. (5) and using the following relations between the aspect ratio and the other variables

$$\sinh 2\Gamma = 2\lambda / (1 - \lambda^2),$$

$$\cosh 2\Gamma = (1 + \lambda^2) / (1 - \lambda^2),$$

one readily finds that the resulting equation involves only the first two Fourier modes in η . It is thus consistent that the second step of the approximation should be to truncate the Fourier expansion of ψ on the ellipse $\xi = \Gamma$ to its first two modes in η . Denoting $\psi_{<2}$ as this truncated streamfunction, we obtain

$$- \frac{\partial \psi_{<2}}{\partial \eta}(\Gamma, \eta) = - \frac{A}{2\pi} \frac{\dot{\lambda}}{\lambda} \cos 2\eta + \frac{1}{2} c^2 \dot{\phi} \sin 2\eta + b \Re [\dot{Z}e^{-i\phi}] \cos \eta + b \Im [\dot{Z}e^{-i\phi}] \sin \eta. \quad (8)$$

The components of order larger than 2 are discarded. In this sense, our formal expansion is a low-order Galerkin-type approximation to full contour dynamics. The remaining task, in the next four sections, is to calculate $\psi_{<2}$ for the various interactions involved in the model. So doing, we exactly retain the part of the motion preserving the elliptical shape.

III. ACTION OF AN EXTERNAL STRAINING FLOW

Let us consider first the effect of uniform strain, of value γ , and background rotation, of value Ω , centered on the origin as shown in Fig. 2. The streamfunction due to this flow is given by

$$\psi = -\frac{1}{4}(\gamma_s z^2 + \gamma_s^* z^{*2}) + \frac{1}{2} \Omega z z^*, \quad (9)$$

where $\gamma_s = \gamma e^{-2i\phi}$, and ϕ_s is the orientation of the strain axes with respect to a fixed frame. The derivative with respect to η on the disk boundary is

$$\begin{aligned} \frac{\partial \psi}{\partial \eta}(\Gamma, \eta) = c \Im [& (-\gamma_s^* Z^* + \Omega Z) e^{-i\phi} \sinh(\Gamma - i\eta)] \\ & - \frac{1}{2} c^2 \Omega \sin 2\eta \\ & + \frac{1}{2} \gamma c^2 (\sinh 2\Gamma \sin 2(\phi - \phi_s) \cos 2\eta \\ & + \cosh 2\Gamma \cos 2(\phi - \phi_s) \sin 2\eta). \end{aligned} \quad (10)$$

This result is obtained without truncation, owing to the fact that ψ is a quadratic function of x and y and does not have angular variations more rapid than 2η . We thus recover the already known result (e.g., Ref. 19) that an external straining flow preserves an elliptical shape. Note that γ , Ω , and ϕ_s may be arbitrary functions of time.

The contributions of this flow to the centroid motion \dot{Z} , the rotation rate $\dot{\phi}$, and the variation of the aspect ratio $\dot{\lambda}$ are obtained by identifying Eq. (10) with the right-hand side of Eq. (8):

$$\dot{Z} \leftarrow -i\gamma_s^* Z^* + i\Omega Z, \quad (11)$$

$$\dot{\phi} \leftarrow \Omega - \gamma \frac{1 + \lambda^2}{1 - \lambda^2} \cos 2(\phi - \phi_s), \quad (12)$$

$$\dot{\lambda} \leftarrow 2\gamma \lambda \sin 2(\phi - \phi_s). \quad (13)$$

A pure strain is obtained with $\Omega = 0$, and a pure shear with $\gamma = \pm \Omega$.

IV. ACTION OF EXTERIOR EMBEDDING DISKS

We now consider the effect of an advecting elliptical disk (Z', λ', ϕ') on an interior advected disk (Z, λ, ϕ). Here and in the next two sections, all primed quantities refer to the

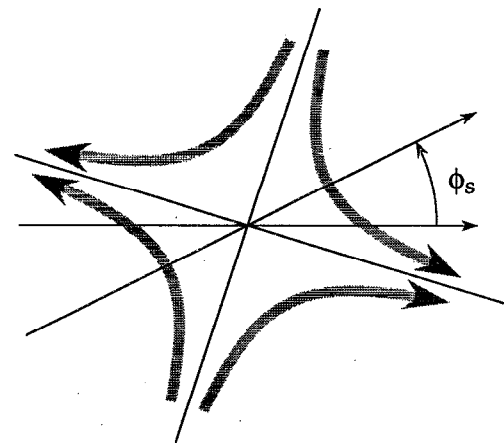


FIG. 2. The strain axes pass through the origin. The bisectrix makes an angle ϕ_s with respect to the x axis.

advactor, while nonprimed quantities refer to the advectee. In the coordinate system linked with the principal axis of the advactor, Eq. (2), the streamfunction may be expressed as:

$$\psi = \frac{1}{2}\omega'(\bar{z}'z'^* - \frac{1}{2}\epsilon'^2(\bar{z}'^2 + z'^2)), \quad (14)$$

with $\epsilon' \equiv \sqrt{(1-\lambda')/(1+\lambda')}$ being the eccentricity of the advactor. The coordinate systems of the advactor and the advectee, both moving with the vorticity disks, are linked by

$$\bar{z}' = \bar{z}e^{i(\phi-\phi')} + (Z-Z')e^{-i\phi'}, \quad (15)$$

hence one may readily obtain ψ as a function of \bar{z} . The differential of ψ with respect to \bar{z} is

$$\frac{\partial\psi}{\partial\bar{z}} = \frac{\omega'}{4} \{ \bar{z}'^* + e^{i\phi}(Z-Z')^* - \epsilon'^2(\bar{z}e^{2i(\phi-\phi')} + (Z-Z')e^{i(\phi-2\phi')}) \},$$

from which, using Eq. (2) again, we obtain

$$\begin{aligned} \frac{\partial\psi}{\partial\eta}(\Gamma, \eta) = & -\frac{1}{2}\omega'c \Im[\sinh(\Gamma+i\eta)e^{i\phi} \\ & \times \{ (Z-Z')^* - \epsilon'^2e^{-2i\phi'}(Z-Z') \}] \\ & + \frac{1}{4}\omega'c^2\{\epsilon'^2 \cos 2(\phi-\phi') \cosh 2\Gamma - 1\} \sin 2\eta \\ & + \frac{1}{4}\omega'c^2\epsilon'^2 \sin 2(\phi-\phi') \sinh 2\Gamma \cos 2\eta \quad (16) \end{aligned}$$

on the advected vortex boundary.

This field, too, is obtained without truncation, and preserves the elliptical shape of the advectee's boundary. The contribution to \dot{Z} , $\dot{\phi}$, and $\dot{\lambda}$ are

$$\dot{Z} \leftarrow \frac{1}{2}i\omega' \{ (Z-Z') - \epsilon'^2e^{2i\phi'}(Z-Z')^* \}, \quad (17)$$

$$\dot{\phi} \leftarrow \frac{1}{2}\omega' \left\{ 1 - \frac{1+\lambda^2}{1-\lambda^2} \epsilon'^2 \cos 2(\phi-\phi') \right\}, \quad (18)$$

$$\dot{\lambda} \leftarrow \omega'\lambda\epsilon'^2 \sin 2(\phi-\phi'). \quad (19)$$

Note that the action of an exterior ellipse and that of a straining flow are closely related. These actions can, in fact, be put into a single form. Comparing the expressions for the streamfunction, Eqs. (9) and (14), the two can be brought into correspondence if we put $\Omega = \frac{1}{2}\omega'$ and $\gamma = \frac{1}{2}\omega'\epsilon'^2$.

We also recover the correct result for the self-advaction of a single Kirchhoff ellipse, when the advectee is identical to the advactor. Then $\dot{\lambda} = 0$ and

$$\dot{\phi} = \omega\lambda / (1+\lambda)^2.$$

V. ACTION OF INTERIOR EMBEDDED DISKS

The case in which the advectee is exterior to the advactor is significantly more complicated but, as we shall see shortly, is still amenable to a closed form analytical solution in terms of elementary functions. The streamfunction outside the advecting ellipse is

$$\psi = \kappa'(\xi' + \frac{1}{2}e^{-2\xi'} \cos 2\eta'), \quad (20)$$

where $\kappa' = A'\omega'/2\pi$ and we recall that (ξ', η') are the radial and azimuthal elliptical coordinates linked to the advactor. Equation (20) matches Eq. (14) on the ellipse boundary up to a constant factor that is irrelevant here.

Since the flow due to the advecting ellipse is irrotational outside its boundary, one may consider that $\psi(z)$ is the real

part of a complex streamfunction $\Psi(z)$ (see Ref. 26, p. 215). Here, Ψ can also be written as a function of $w' = \xi' + i\eta'$ and the complex form of Eq. (20) is

$$\Psi = \kappa'(w' + \frac{1}{2}e^{-2w'}). \quad (21)$$

The complex elliptical coordinate $w = \xi + i\eta$ linked to the advectee is related to w' by

$$Z + 2\nu \cosh w = Z' + 2\nu' \cosh w',$$

with $\nu \equiv \frac{1}{2}ce^{i\phi}$. Thus we also have

$$\frac{dw'}{dw} = \Lambda \frac{\sinh w}{\sinh w'},$$

with $\Lambda \equiv \nu/\nu'$ and we can differentiate Ψ with respect to w to obtain

$$\frac{\partial\Psi}{\partial w} = 2\Lambda\kappa'e^{-w'} \sinh w. \quad (22)$$

It is easy to see that the imaginary part of Eq. (22), $-\partial\Psi/\partial\eta$, does not contain terms varying more rapidly than $\cos 2\eta$ and $\sin 2\eta$ on the boundary $\xi = \Gamma$ of the advectee if and only if the two ellipses possess the same foci. In this case, we have $w \equiv w'$, and the contributions to \dot{Z} and $\dot{\lambda}$ vanish while the contribution to $\dot{\phi}$ is given by

$$\dot{\phi} \leftarrow 2\kappa' \frac{\pi}{A} \frac{\lambda}{(1+\lambda)^2}.$$

Generally, $\partial\psi/\partial\eta$ on $\xi = \Gamma$ may be written as a Fourier series in η :

$$-\frac{\partial\psi}{\partial\eta}(\Gamma, \eta) = \sum_{m=1}^{\infty} (I_m \sin m\eta + J_m \cos m\eta). \quad (23)$$

All terms with $m > 2$ are discarded under our basic assumption and the remaining terms are used with Eq. (8) to obtain the contributions to the evolution of the advectee. The quantities I_m and J_m can be computed by two contour integrals along the advectee's boundary:

$$I_m = -\frac{1}{\pi} \int_0^{2\pi} \frac{\partial\psi}{\partial\eta} \sin m\eta \, d\eta,$$

$$J_m = -\frac{1}{\pi} \int_0^{2\pi} \frac{\partial\psi}{\partial\eta} \cos m\eta \, d\eta.$$

It is easier to handle these integrals in their complex representation, in which

$$\begin{aligned} J_m + iI_m = & -\frac{1}{2\pi} \left[\int_{\Gamma}^{\Gamma+2i\pi} \frac{\partial\Psi}{\partial w} e^{m(w-\Gamma)} \, dw \right. \\ & \left. + \left(\int_{\Gamma}^{\Gamma+2\pi i} \frac{\partial\Psi}{\partial w} e^{-m(w-\Gamma)} \, dw \right)^* \right] \quad (24) \end{aligned}$$

$$\begin{aligned} = & -\frac{1}{2\pi} \left[\frac{\kappa'}{\nu'} \oint_C e^{-w'+m(w-\Gamma)} \, dz \right. \\ & \left. + \left(\frac{\kappa'}{\nu'} \oint_C e^{-w'-m(w-\Gamma)} \, dz \right)^* \right], \quad (25) \end{aligned}$$

where C is the boundary of the advectee.

The integrands are multivalued functions of z with branch cuts on the segments connecting the two pairs of foci. The integration contour around the exterior disk encompasses these two cuts and there do not exist other branch cuts or poles at finite distance outside the integration contour. In addition, it is shown below that the Laurent series in z of the

integrands have an algebraic bound (i.e., do not diverge faster than a polynomial). Thus J_m and I_m can be computed along a closed contour that tends to infinity, and it is sufficient for that to get the $1/z$ term in the Laurent series of the integrands. One finds easily that the second integrand in Eq. (25) behaves as dz/z^{m+1} , so that the second integral is zero for $m > 0$. The first integral is calculated using a further change of coordinate, from w to \bar{z}' . The expansion of the exponential terms as a Laurent series in \bar{z} and \bar{z}' is derived from Eq. (2). We obtain

$$e^{-w} = \frac{c'}{2\bar{z}'} + \frac{c'^3}{8\bar{z}'^3} + \frac{c'^5}{16\bar{z}'^5} + \dots,$$

$$e^w = \frac{2\bar{z}}{c} - \frac{c}{2\bar{z}} - \frac{c^3}{8\bar{z}^3} - \dots,$$

$$e^{2w} = \frac{4\bar{z}^2}{c^2} - 2 - \frac{c^2}{4\bar{z}^2} - \dots.$$

Using Eq. (15), we eliminate \bar{z} and obtain

$$e^{w-w'} = \dots - \frac{c'(Z-Z')}{2\sqrt{Z'}} + \dots,$$

$$e^{2w-w'} = \dots + \left(\frac{c'(Z-Z')^2}{2\sqrt{Z'}} + \frac{c'}{2\Lambda^2} - c' \right) \frac{1}{\bar{z}'} + \dots.$$

Therefore

$$J_1 + iI_1 = i \frac{\kappa'}{\nu} e^{-\Gamma(Z-Z')}, \quad (26)$$

$$J_2 + iI_2 = -i \frac{\kappa'}{\nu^2} e^{-2\Gamma(Z-Z')} - i\kappa'(1/\Lambda^2 - 2)e^{-2\Gamma}. \quad (27)$$

The J_m and I_m for $m > 2$ are needed in Part II and can be computed in the same way.

From Eqs. (26) and (27) and using Eq. (8), a few algebraic manipulations lead to the required contributions to the evolution of the advectee:

$$\dot{Z} \leftarrow \frac{i\pi\kappa'}{A} \{ (Z-Z') - \epsilon^2 e^{2i\phi} (Z-Z')^* \}, \quad (28)$$

$$\begin{aligned} \dot{\phi} \leftarrow & \frac{8\pi^2\kappa'}{A^2} \frac{\lambda^2}{(1-\lambda^2)(1+\lambda)^2} \Re[(Z-Z')^2 e^{-2i\phi}] \\ & + \omega' \frac{A'\lambda}{A(1+\lambda)^2} \left(2 - \frac{A'\lambda(1-\lambda'^2)}{A\lambda'(1-\lambda^2)} \cos 2(\phi - \phi') \right), \end{aligned} \quad (29)$$

$$\begin{aligned} \dot{\lambda} \leftarrow & \frac{8\pi^2\kappa'}{A^2} \frac{\lambda^2}{(1+\lambda)^2} \Im[(Z-Z')^2 e^{-2i\phi}] \\ & + \omega' \frac{A'^2\lambda^2(1-\lambda'^2)}{A^2\lambda'(1+\lambda)^2} \sin 2(\phi - \phi'). \end{aligned} \quad (30)$$

The case of a single Kirchhoff ellipse is again obtained in the limit when the advector is identical to the advectee.

VI. ACTION OF SEPARATED DISKS

We now add the final stage of complexity by considering the interaction between separated vortices. At first sight this case does not appear more complicated than the one treated in the last section, so one would expect very similar calculations to apply. A serious difficulty, however, arises in the

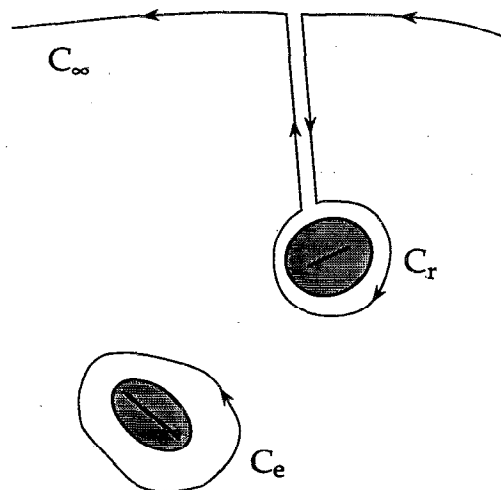


FIG. 3. The figure shows the disk boundaries and the branch cuts connecting the foci when the two disks are separated. It also shows why the contour C_e around the advectee is not homeomorphic to a contour at infinity C_∞ as when the advector is embedded within the advectee but encounters the advector around the contour C_r .

calculation of I_m and J_m : the branch cut of the advector in the z plane is now exterior to the advectee, and hence it is no longer possible to obtain the two integrals as a residue on a contour at infinity. As illustrated in Fig. 3, one cannot avoid integrating around one of the two branch cuts. As a consequence, the integrals cannot be reduced to a combination of elementary functions but are complete elliptic integrals of the third type with complex modulus and arguments. After some transformations, a closed form expression can be obtained in terms of Weierstrass elliptic functions. This expression is not, however, particularly useful and we thus turn towards an approximate calculation of this interaction with more physical insight.

The approximation to be used consists of replacing the effect of the advector by the effect of a *finite* number of point

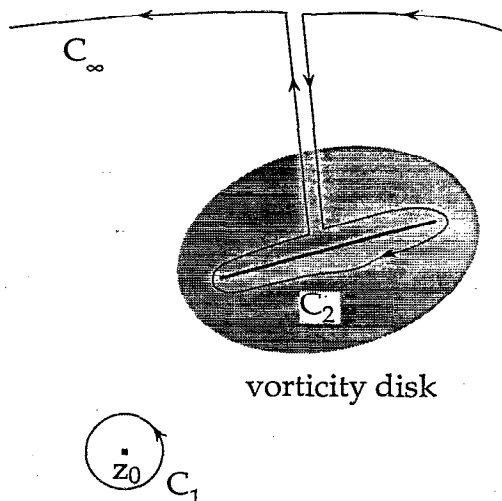


FIG. 4. The contour C_1 is homeomorphic to the combination of the contours C_∞ and C_2 needed for the computation of the velocity at z_0 due to the vorticity disk. Since the integral around C_∞ cancels (see text), the vorticity disk can be replaced by a sheet distribution of vorticity along the segment connecting the two foci.

vortices whose strengths and locations are chosen to obtain the most accurate results possible. This approach is based on the equivalence between an ellipse of uniform vorticity and a vortex sheet with a particular strength distribution connecting the two foci of the ellipse. This result, which is apparently new, is easily established for the complex velocity field at any point z_0 exterior to the advecting ellipse (Z, λ, ϕ) . First applying the Cauchy theorem to the contour C_1 surrounding z_0 (see Fig. 4), we obtain

$$\frac{\partial \Psi}{\partial z}(z_0) = \frac{\kappa}{\nu} e^{-w(z_0)} = -\frac{i\kappa}{2\pi\nu} \oint_{C_1} \frac{e^{-w(z)}}{z - z_0} dz. \quad (31)$$

By deforming this contour as shown in Fig. 4, one may compute the integral around C_1 from a sum of two integrals, one taken around the contour at infinity, C_∞ , and the other around the contour C_2 surrounding the branch cut connecting the two foci of the ellipse. That is,

$$\oint_{C_1} = \oint_{C_\infty} - \oint_{C_2}.$$

The integral around C_∞ cancels because $e^{-w} \sim \nu/z$ there, so we are left with

$$\frac{\partial \Psi}{\partial z}(z_0) = \frac{i\kappa}{2\pi\nu} \oint_{C_2} \frac{e^{-w}}{z - z_0} dz, \quad (32)$$

or exactly the velocity field induced by a vortex sheet having the strength distribution

$$\mu(s) = \frac{2\kappa}{\pi c} \sqrt{1 - s^2}, \quad -1 \leq s \leq 1,$$

where s parametrizes the segment connecting the two foci of the ellipse. Thus,

$$\Psi(z) = \int_{-1}^{+1} c \mu(s) \log(z - Z - 2vs) ds. \quad (33)$$

Note:

(1) This result is only valid for the domain outside the ellipse; this representation is not valid inside where the velocity field is rotational.

(2) As this representation is purely static, the evolution of the vortex is not exactly given by the velocity on the vorticity sheet between the two foci. We show later in this section that this velocity provides, though, a very good approximation of the vortex motion.

(3) This result can be generalized to an advecting vortex of any shape provided one knows the branch cuts of the conformal transform mapping the vortex boundary onto a circle. The vortex can be replaced by vortex sheets along the cuts of the Riemann surface which induce the same distribution of velocity outside the vortex.

Having shown that the vortex can be exactly replaced by a single sheet, an accurate approximation can be obtained by discretizing the vorticity sheet as a family of point vortices. It is shown in Appendix A that an optimal discretization in K vortices is obtained by placing vortices at the locations

$$s_k = \cos(\pi k / (K + 1)), \quad (34)$$

and assigning them strengths

$$\mu_k \kappa = \frac{2\kappa}{K + 1} (1 - s_k^2), \quad (35)$$

for $k = 1, 2, \dots, K$.

The effect of the advector on the advectee is approximated by summing the effects of the corresponding point vortices. These effects superpose, so it is only necessary to consider the effect of one point vortex for the moment. Let the strength of this point vortex be denoted κ_\odot and its position denoted z_\odot . The effect of this point vortex on the advectee is calculated from the integrals I_m and J_m defined by Eq. (25). The calculation is made in Appendix B and we obtain

$$I_m = -2\kappa_\odot \cosh m \Gamma \Re[e^{-m\tilde{w}_\odot}], \quad (36)$$

$$J_m = -2\kappa_\odot \sinh m \Gamma \Im[e^{-m\tilde{w}_\odot}]. \quad (37)$$

where \tilde{w}_\odot is the location of the point vortex in the elliptical coordinates of the advectee.

The complete effect of the advector on the advectee, therefore, is given by replacing $I_1, J_1, I_2,$ and J_2 in Eqs. (23) by their expressions in Eqs. (36) and (37) summed over the number of point vortices, with $\kappa_\odot = \mu_k \kappa'$, $\tilde{w}_\odot = \tilde{w}_k$, and $z_\odot = Z' + s_k c' e^{i\phi} = Z + c e^{i\phi} \cosh \tilde{w}_k$ for $k = 1, 2, \dots, K$.

We can now give the contribution of a separated advector to the motion of the advectee:

$$\dot{Z} \leftarrow -\frac{ik'}{\nu^*} \sum_{k=1}^K \mu_k e^{-\tilde{w}_k^*}, \quad (38)$$

$$\dot{\phi} \leftarrow -2\omega' \frac{A'}{A} \frac{\lambda(1 + \lambda^2)}{(1 - \lambda^2)^2} \sum_{k=1}^K \mu_k \Re[e^{-2\tilde{w}_k}], \quad (39)$$

$$\dot{\lambda} \leftarrow +4\omega' \frac{A'}{A} \frac{\lambda^2}{(1 - \lambda^2)} \sum_{k=1}^K \mu_k \Im[e^{-2\tilde{w}_k}]. \quad (40)$$

Note that the previous model of MZS^{20,27} can be recovered by representing the advector by a single point vortex at its center and by keeping only the leading terms in the corresponding version of Eqs. (38)–(40) up to order 3 in $\Delta Z = Z' - Z$. We then have

$$\dot{Z} \leftarrow -\frac{ik'}{\Delta Z^*} - \frac{ik'A(1 - \lambda^2)e^{-2i\phi}}{\pi\lambda\Delta Z^*3},$$

$$\dot{\phi} \leftarrow -\omega' \frac{A'}{2\pi} \frac{1 + \lambda^2}{1 - \lambda^2} \Re \left[\frac{e^{2i\phi}}{\Delta Z^2} \right],$$

$$\dot{\lambda} \leftarrow +\omega' \frac{A'}{\pi} \lambda \Im \left[\frac{e^{2i\phi}}{\Delta Z^2} \right].$$

These contributions are identical to the coupling terms in Eqs. (3.19), (3.20), and (3.24) of MZS. The present method therefore represents the full extension of the second-order moment model, enabling us to recover the exact elliptical results to any accuracy desired.

The neglected terms in the elliptical assumption arise from I_m and J_m with $m > 2$. It is shown from Eqs. (36) and (37) that these terms vary as $(Z - Z')^{-m}$ and, thus, can be neglected for large enough separation.

It is shown in the following paper²⁵ that Eqs. (38)–(40), with as few as five point vortices used in the representation of a given disk, produce very satisfactory results in a number of illustrative cases when compared with reference solutions obtained with contour dynamics. Unfortunately, these equations also possess the undesirable property, established in the following section, that the global centroid, the angular impulse and the kinetic energy are not exactly conserved by the motion. These quantities are invariants of the original problem and it is desirable to preserve their conser-

vation in any approximate model, especially if one is interested in statistical properties or in Hamiltonian structure (see next section). Nonconservation in Eqs. (38)–(40) is basically due to the lack of symmetry in the approximation applied: the advectee is treated exactly while the advector is represented as a series of point vortices. Symmetry is reestablished, and conservation follows, as we shall see in the following section, if the advectee is submitted to the same level of approximation as the advector. In practice, one has to expand $e^{-\tilde{w}_k}$ just as we had $e^{-w'}$ (see Appendix A), i.e.,

$$e^{-\tilde{w}_k} \approx \frac{1}{2} \sum_{l=1}^K \frac{\mu_l}{\cosh \tilde{w}_k - s_l} = \sum_{l=1}^K \frac{\mu_l \nu}{(Z' - Z) + 2s_k \nu' - 2s_l \nu}. \quad (41)$$

Using the same discretization, we obtain the following approximation for $e^{-2\tilde{w}_k}$:

$$e^{-2\tilde{w}_k} \approx \sum_{l=1}^K \frac{\mu_l s_l}{\cosh \tilde{w}_k - s_l} = \sum_{l=1}^K \frac{2\mu_l s_l \nu}{(Z' - Z) + 2s_k \nu' - 2s_l \nu}. \quad (42)$$

Note the error term in Eq. (41) is of the type given in Eq. (A10) but this is not the case in Eq. (42). An optimal representation of $e^{-2\tilde{w}_k}$ would require a different distribution of points between the two foci.

Replacing $e^{-\tilde{w}_k}$ and $e^{-2\tilde{w}_k}$ by the above expressions, Eqs. (38)–(40) become

$$\dot{Z} \leftarrow -ik' \sum_{k=1}^K \sum_{l=1}^K \frac{\mu_k \mu_l}{(Z' - Z)^* + 2s_k \nu'^* - 2s_l \nu'^*}, \quad (43)$$

$$\dot{\phi} \leftarrow -4\omega' \frac{A'}{A} \frac{\lambda(1+\lambda^2)}{(1-\lambda^2)^2} \sum_{k=1}^K \sum_{l=1}^K \mu_k \mu_l s_l \times \Re \left[\frac{\nu}{(Z' - Z) + 2s_k \nu' - 2s_l \nu} \right], \quad (44)$$

$$\dot{\lambda} \leftarrow +8\omega' \frac{A'}{A} \frac{\lambda^2}{(1-\lambda^2)} \sum_{k=1}^K \sum_{l=1}^K \mu_k \mu_l s_l \times \Im \left[\frac{\nu}{(Z' - Z) + 2s_k \nu' - 2s_l \nu} \right]. \quad (45)$$

VII. INVARIANTS OF MOTION

For a family of nonaxisymmetric distributed vortices, the two-dimensional Euler equations possess a series of global invariants all of which are preserved by the elliptical model.

We first observe that the total vorticity and the integral of any functional of the vorticity over a given disk are conserved by the very hypothesis the model is based on. We cannot, however, refer to vorticity conservation for each particle, because the particles located between two contiguous ellipses are indistinguishable. Such a notion is reestablished in the limit where the increment of each disk is infinitesimal and the vorticity profile becomes continuous.

In order to establish the conservation of the vorticity

centroid, the angular impulse, and the total energy, it is most convenient to observe that the model can be described as a set of conjugate Hamiltonian equations. For each of the interactions described in Secs. III–VI, the evolution equations can be deduced from an associated elementary Hamiltonian. We must here consider the auto-advection of a disk as a separate case, but we can group together the cases of an exterior embedding disk and of an interior embedded disk into a single case. Hence we are left with only four cases. The elementary Hamiltonians are as follows.

(1) Auto-advection of a single elliptical disk:

$$\mathcal{H}_0 = \frac{1}{2} \pi \kappa^2 \log \frac{(1+\lambda)^2}{\lambda}. \quad (46)$$

(2) Interaction with an external straining flow (Sec. III):

$$\mathcal{H}_1 = -\frac{\pi \gamma}{8\kappa} e^{2i\phi_s} Z^{*2} - \frac{A \gamma \kappa}{4} \left(\frac{1}{\lambda} - \lambda \right) \cos 2(\phi - \phi_s) + \frac{\pi \Omega}{16\kappa} |Z|^2 + \Omega \frac{A \kappa}{4} \left(\frac{1}{\lambda} + \lambda \right). \quad (47)$$

(3) Interaction of two embedded elliptical disks (Secs. IV and V) where the primed disk is the internal one:

$$\mathcal{H}_2 = \frac{\pi \omega \kappa'}{2} \{ |Z - Z'|^2 - \epsilon^2 \Re[(Z - Z')^2 e^{-2i\phi}] \} + \pi \kappa \kappa' \log \frac{(1+\lambda)^2}{\lambda} - \frac{\pi \kappa \kappa' A'}{4 A} \left(\lambda' + \frac{1}{\lambda'} \right) - \frac{\pi \kappa \kappa' A'}{4 A} \epsilon^2 \left(\frac{1}{\lambda'} - \lambda' \right) \cos 2(\phi - \phi'). \quad (48)$$

(4) Interaction of two separated elliptical disks [Sec. VI, Eqs. (43)–(45)]:

$$\mathcal{H}_3 = \Re \left[2\pi \kappa \kappa' \sum_{k=1}^K \sum_{l=1}^K \mu_k \mu_l \times \log(Z' - Z + 2s_k \nu' - 2s_l \nu) \right]. \quad (49)$$

From the above expressions, one may verify that the evolution equations described in Secs. III–VII can be recovered as

$$\dot{Z} = \frac{i}{2\pi \kappa} \left(\frac{\partial \mathcal{H}_i}{\partial Z} \right)^*, \quad (50)$$

$$\frac{A \kappa}{4} \left(\frac{1}{\lambda^2} - 1 \right) \dot{\phi} = -\frac{\partial \mathcal{H}_i}{\partial \lambda}, \quad (51)$$

$$\frac{A \kappa}{4} \left(\frac{1}{\lambda^2} - 1 \right) \dot{\lambda} = +\frac{\partial \mathcal{H}_i}{\partial \phi}. \quad (52)$$

Note \mathcal{H}_3 is identical to the Hamiltonian coupling the two families of point vortices used in the representation of the two vortices. But the point vortices are not free to move independently; they are linked in a collective state described by the discretization (34), in which the only degrees of freedom are Z , λ , and ϕ .

The total Hamiltonian \mathcal{H} for a system of distributed vortices is obtained as the sum of the elementary Hamiltonians for all possible couplings. It can be written symbolically as follows:

$$\mathcal{H} = \sum_{\text{all disks}} (\mathcal{H}_0 + \mathcal{H}_1) + \sum_{\text{all couples of embedded disks}} \mathcal{H}_2 + \sum_{\text{all couples of separated disks}} \mathcal{H}_3.$$

It is clear from Eqs. (50)–(52) that \mathcal{H} is the excess kinetic energy of the system.¹⁶

The global vorticity centroid is defined as

$$\mathcal{Z} = \frac{\sum_{\text{all disks}} \kappa Z}{\sum_{\text{all disks}} \kappa}.$$

This quantity is conserved by the combination of Eqs. (17) and (28) for a couple of embedded disks; it is also conserved by Eq. (43) for a couple of separated disks [this is not true using Eq. (38) except in the limit $K \rightarrow \infty$]. Note it is important that all vortices be discretized with the same number of points. Nonzero external strain does not conserve the global centroid.

One can see from Eqs. (51) and (52) that λ and ϕ are not canonical variables for \mathcal{H} . Canonical variables p and q can be obtained here from λ and ϕ by a change of variables satisfying

$$\frac{\partial p}{\partial \phi} \frac{\partial q}{\partial \lambda} - \frac{\partial p}{\partial \lambda} \frac{\partial q}{\partial \phi} = \frac{A\kappa}{4} \left(\frac{1}{\lambda^2} - 1 \right). \quad (53)$$

One choice of particular interest is

$$p = \frac{1}{8} A\kappa (1/\lambda + \lambda), \quad (54)$$

$$q = 2\phi, \quad (55)$$

for which

$$\dot{p} = -\frac{1}{2} \frac{\partial \mathcal{H}}{\partial \phi}.$$

We obtain a simple expression for the total angular impulse in terms of Z and p ,

$$\mathcal{I} \equiv \iint \omega(x^2 + y^2) dx dy = \sum_{\text{all disks}} (2\pi\kappa |Z|^2 + 4p), \quad (56)$$

from which we can show by a straightforward calculation that the elementary Hamiltonians \mathcal{H}_0 , \mathcal{H}_2 , and \mathcal{H}_3 conserve \mathcal{I} . Nonzero external strain breaks conservation of \mathcal{I} as well.

Another choice of canonical coordinates is useful for numerical purposes. It was observed by MZS that either (λ, ϕ) or the above choice of canonical coordinates are singular when λ becomes equal to 1. These authors introduced the following set of nonsingular canonical coordinates:

$$(D, G) = (\kappa A / 4\lambda)^{1/2} (1 - \lambda) (\cos 2\phi, \sin 2\phi).$$

The singularity can also be removed using the complex non-canonical coordinate $\frac{1}{2} c^2 e^{-2i\phi}$ for which particularly useful simplifications occur in the equations. The derivation of the corresponding equations is left as an exercise for the reader.

VIII. DISCUSSION AND CONCLUSION

The elliptical model of two-dimensional vortex dynamics approximates the evolution of a family of distributed vortices immersed in an external straining field. It is based on a Lagrangian formulation of the dynamics of the vorticity contours of vortices that are assumed to remain elliptical for

all time. We have limited the scope of this paper to a comprehensive presentation of the various types of interactions involved in the elliptical model. The assembly of all contributions into a single set of equations is performed in the following paper.²⁵

The assumption that vorticity contours remain close to ellipses is *a priori* valid only when the contours of a given distributed vortex are almost confocal and when separated vortices are far apart. The nonlinear effects of neglected terms cannot be, however, easily determined within the framework of the elliptical model. The practical utility of the model and its advantages with respect to existing formulation are established by the results of a series of numerical tests, presented in Ref. 25, in which the elliptical model is compared with state-of-the-art contour dynamics.

The present model is a step en route to an approximation theory of vortex dynamics. The following paper²⁵ describes an extension to small perturbations of the elliptical shapes. The incorporation of finite nonelliptical deformations requires a generalization of the conformal transform used here in order to deal with higher-order deformations.²⁹ A clear limitation of the elliptical model lies in the problem of stripping and filamentation.^{22,28} Although stripped filaments of vorticity are not explicitly described within the model, they could be handled by computing the location of comoving critical points and appropriately removing the exterior vorticity contours of the vortex. Work in these directions is currently in progress.

This model and its future extensions are potentially useful as a theoretical apparatus for the investigation of vortex dynamics and as a tool for the interpretation of numerous experimental structures, such as the vortices produced in shear layers to name but one. The model provides a compact, simple representation of the essential features of a flow dominated by coherent vortices.

ACKNOWLEDGMENTS

We are grateful to C. Basdevant and N. J. Zabusky for valuable discussions and repeated encouragements. We thank F. Pascal for his careful reading and several corrections.

APPENDIX A: OPTIMAL DISCRETIZATION OF THE VORTEX SHEET

Consider the problem of finding the locations and strengths of K point vortices that represent the exterior velocity of the advector as accurately as possible. Let $\mu_1, \mu_2, \dots, \mu_K$ denote the dimensionless strengths of the point vortices and s_1, s_2, \dots, s_K denote the dimensionless positions (made dimensionless on c). Then the point vortex representation of the complex velocity due to this distribution is given by

$$\frac{\partial \Psi}{\partial w'} = 2\kappa' \sinh w' E(w'),$$

with

$$E(w') = \frac{1}{2} \sum_{k=1}^K \frac{\mu_k}{\cosh w' - s_k},$$

and where we use the elliptical coordinate system linked with the advectee.

We want to choose the μ_k and s_k to make $E(w')$ as close as possible to the exact value, $e^{-w'}$. Symmetry dictates that the μ_k should be distributed symmetrically with respect of the center of the vortex and the s_k antisymmetrically. As a consequence, $E(w')$ has the expansion $E(w') = e^{-w'} + c_3 e^{-3w'} + c_5 e^{-5w'} + \dots$, so the object is to choose the μ_k and s_k in such a way as to annihilate as many higher-order terms in the expansion of $E(w')$ as possible. For K vortices, we can annihilate $K - 1$ terms; formally, we do this by demanding

$$\int_{\varepsilon}^{\varepsilon + 2\pi i} E(w') e^{(2m+1)w'} dw' = 0, \quad m = 1, 2, \dots, K - 1 \quad (\text{A1})$$

and

$$\frac{1}{2\pi i} \int_{\varepsilon}^{\varepsilon + 2\pi i} E(w') e^{w'} dw' = 1, \quad (\text{A2})$$

where ε is an arbitrary real positive quantity. With the substitution $u = e^{w'}$, Eqs. (A1) and (A2) may be evaluated on a closed contour using the calculus of residues, leaving

$$\sum_{k=1}^K \mu_k \frac{z_{+k}^{2m+1} - z_{-k}^{2m+1}}{z_{+k} - z_{-k}} = \delta_{m0}, \quad (\text{A3})$$

where δ_{mn} is the Kronecker delta symbol, and

$$z_{\pm k} = s_k \pm i\sqrt{1 - s_k^2} \equiv e^{\pm i\varphi_k}. \quad (\text{A4})$$

The division in Eq. (A3) is easily carried out, and we are left with the sequence of conditions

$$\sum_{k=1}^K \mu_k = 1, \quad (\text{A5})$$

$$\sum_{k=1}^K \mu_k \cos 2\varphi_k = -\frac{1}{2}, \quad (\text{A6})$$

$$\sum_{k=1}^K \mu_k \cos 2m\varphi_k = 0, \quad m = 2, 3, \dots, K - 1. \quad (\text{A7})$$

Remarkably, these conditions are satisfied by $\varphi_k = \pi k / (K + 1)$ and $\mu_k = 2 \sin^2 \varphi_k / (K + 1)$, or

$$s_k = \cos \frac{\pi k}{K + 1}, \quad (\text{A8})$$

$$\mu_k = \frac{2}{K + 1} (1 - s_k^2), \quad (\text{A9})$$

for $k = 1, 2, \dots, K$.

The leading-order error term $\int_{\varepsilon}^{\varepsilon + 2i\pi} E(w') e^{(2K+1)w'} dw'$ is easily evaluated along the same lines. It is

$$\sum_{k=1}^K \mu_k (z_{+k}^{2K} + z_{-k}^{2K}) = 2 \sum_{k=1}^K \mu_k \cos 2K\varphi_k = -1.$$

Hence,

$$E(w') = e^{-w'} (1 - e^{-2Kw'} + \dots). \quad (\text{A10})$$

This last result shows that the point vortex approximation has excellent convergence properties. In terms of the z' variable, we have retained the first $2K$ terms in the Laurent series of the velocity field.

APPENDIX B: EFFECT OF A SINGLE VORTEX ON A SEPARATED ELLIPSE

The effect of a single point vortex ($z_{\odot}, \kappa_{\odot}$) on a separated ellipse can be computed using Eq. (24) again. Now Ψ is the streamfunction due to the single vortex, and we pass to z coordinates by

$$\frac{\partial \Psi}{\partial w} dw = \kappa_{\odot} \frac{dz}{z - z_{\odot}}.$$

The integration is performed around the boundary of the advectee. We thus have to sum a contribution from the contour at infinity, as we did in Sec. V, with a residue at each vortex location. The contribution at infinity is obtained from the asymptotic behavior of $e^{-mw}/(z - z_{\odot})$ and $e^{mw}/(z - z_{\odot})$. The first quantity is of order $1/z^{m+1}$, so the second integral in Eq. (24) again does not produce any contribution from infinity. The second quantity does have a term of order $1/z$. It can be determined by first noting, from Eq. (1), that e^{mw} can be written as

$$e^{mw} = P(z) + R(z^{-1}),$$

where P is a polynomial of order m and R is an integer series with zero constant term. Thus, the principal term in $e^{mw}/(z - z_{\odot})$ is $P(z_{\odot})/z$. Now, note that since $\cosh mw$ is a polynomial in z and $\cosh mw - \sinh mw = O(1/z^m)$, we have

$$\cosh mw = \frac{1}{2}P(z)$$

and

$$\sinh mw = \frac{1}{2}P(z) + R(z^{-1}).$$

As a consequence, we obtain the contribution

$$\begin{aligned} J_m + iI_m &\leftarrow -\frac{\kappa_{\odot}}{2\pi} e^{-m\Gamma} \oint_{C_{\infty}} \frac{e^{mw}}{z - z_{\odot}} dz \\ &= -2i\kappa_{\odot} e^{-m\Gamma} \cosh m\tilde{w}_{\odot}, \end{aligned} \quad (\text{B1})$$

where \tilde{w}_{\odot} is the location of the point vortex in the elliptical coordinates of the advectee; it is determined from the solution of

$$Z + ce^{i\phi} \cosh \tilde{w}_{\odot} = z_{\odot},$$

which can be put in the form of a quadratic equation for $e^{-\tilde{w}_{\odot}}$.

In addition, from Eq. (24), the residues at each vortex location give the contribution

$$J_m + iI_m \leftarrow i\kappa_{\odot} (e^{-m\Gamma} e^{m\tilde{w}_{\odot}} - e^{m\Gamma} e^{-m\tilde{w}_{\odot}}). \quad (\text{B2})$$

Combining Eqs. (B1) and (B2), we obtain

$$I_m = -2\kappa_{\odot} \cosh m\Gamma \Re[e^{-m\tilde{w}_{\odot}}], \quad (\text{B3})$$

$$J_m = -2\kappa_{\odot} \sinh m\Gamma \Im[e^{-m\tilde{w}_{\odot}}]. \quad (\text{B4})$$

¹R. Benzi, S. Patarnello, and P. Santangelo, J. Phys. A: Math. Gen. **21**, 1221 (1988).

²P. Santangelo, R. Benzi, and B. Legras, Phys. Fluids A **1**, 1027 (1989).

³B. Legras, P. Santangelo, and R. Benzi, Europhys. Lett. **5**, 37 (1988).

⁴B. Fornberg, J. Comput. Phys. **25**, 1 (1977).

⁵C. Basdevant, B. Legras, R. Sadourny, and M. B eland, J. Atmos. Sci. **38**, 2305 (1981).

⁶J. C. McWilliams, J. Fluid. Mech. **146**, 21 (1984).

- ⁷E. J. Hopfinger, F. K. Browand, and Y. Gagne, *J. Fluid Mech.* **125**, 505 (1982).
- ⁸Y. Couder and C. Basdevant, *J. Fluid Mech.* **173**, 225 (1986).
- ⁹A. I. Ginzburg, A. G. Kostyanoy, A. M. Pavlov, and K. N. Fedorov, *Izv. Atmos. Ocean. Phys.* **23**, 128 (1987).
- ¹⁰J. M. Nguyen Duc and J. Sommeria, *J. Fluid Mech.* **192**, 175 (1988).
- ¹¹G. J. F. Van Heijst and J. B. Flor, *Nature* **340**, 212 (1989).
- ¹²N. J. Zabusky, M. H. Hughes, and K. V. Roberts, *J. Comput. Phys.* **30**, 96 (1979).
- ¹³D. G. Dritschel, *Comp. Phys. Rep.* **10**, 77 (1989) and references herein.
- ¹⁴G. S. Deem and N. J. Zabusky, *Phys. Rev. Lett.* **40**, 859 (1978).
- ¹⁵R. T. Pierrehumbert, *J. Fluid Mech.* **99**, 129 (1980).
- ¹⁶D. G. Dritschel, *J. Fluid Mech.* **157**, 95 (1985).
- ¹⁷H. H. Lamb, *Hydrodynamics* (Dover, New York, 1932).
- ¹⁸D. W. Moore and P. G. Saffman, in *Aircraft Wake Turbulence and Its Detection*, edited by J. Olsen, A. Goldberg, and N. Rogers (Plenum, New York, 1971).
- ¹⁹S. Kida, *J. Phys. Soc. Jpn.* **50**, 3517 (1981).
- ²⁰M. V. Melander, N. J. Zabusky, and A. S. Styczek, *J. Fluid Mech.* **167**, 95 (1986).
- ²¹D. G. Dritschel, in *Mathematical Aspects of Vortex Dynamics*, edited by R. E. Caflisch (Society for Industrial and Applied Mathematics, Philadelphia, 1989), Chap. 10.
- ²²D. G. Dritschel and B. Legras (in preparation, 1991).
- ²³G. K. Batchelor, *An Introduction to Fluid Dynamics* (Cambridge U.P., Cambridge, 1967), p. 535.
- ²⁴M. V. Melander, J. C. McWilliams, and N. J. Zabusky, *J. Fluid Mech.* **178**, 137 (1987).
- ²⁵D. G. Dritschel and B. Legras, *Phys. Fluids A* **3**, 855 (1991).
- ²⁶P. M. Morse and H. Feshbach, *Methods of Theoretical Physics* (McGraw-Hill, New York, 1953).
- ²⁷A. A. Abrashkin, *Fluid Dyn.* **1**, 53 (1987).
- ²⁸D. G. Dritschel, *J. Fluid Mech.* **194**, 511 (1988).
- ²⁹B. Legras and D. G. Dritschel, in *Proceedings of the IMA Workshop on Nonlinear Phenomena in Atmospheric and Oceanic Sciences*, IMA volumes in Mathematics and its Applications (Springer-Verlag, Berlin, in press).